Climatic Change (2010) 99:247–259
DOI 10.1007/s10584-009-9658-3

Warming of an elevated layer over the Caribbean

Mark R. Jury · Amos Winter

Received: 7 February 2008 / Accepted: 29 May 2009 / Published online: 12 September 2009

Abstract Air temperatures in the trade wind inversion (~850 hPa) over the Caribbean have been rising much faster than sea temperatures. This is associated with an accelerated Hadley circulation, with sinking motions over the Caribbean corresponding with increasing rising motion over the Amazon. The sinking motions induce a faster rate of warming and drying in the trade wind inversion than at other levels. Much of the trend in Caribbean climate is attributable to physical mechanisms; changes in atmospheric composition play a secondary role. Smoke and dust plumes from Africa, drifting westward across the Atlantic, enhance the greenhouse effect in an elevated (1–3 km) layer. A stabilized lower atmosphere across the Caribbean has contributed to warming and drying trends over the twentieth century which are projected to continue. The atmosphere is warming faster than the ocean, causing a decline in sensible heat fluxes that fuel tropical cyclones.

1 Introduction

The Hadley cell is a prominent feature of the general circulation of the tropical atmosphere. Subsidence in the Hadley cell plays an important role in determining the position and intensity of the subtropical dry zones. Ground- and satellite-based observations (Fu et al. 2006) and recent model simulations (IPCC 2007) reveal a recent meridional widening and poleward shift of the Hadley cell (Frierson et al. 2007). The northward shift of the Hadley cell together with global warming is likely to cause intensification of storm tracks in mid latitudes (Bengtsson et al. 2006), expansion of the subtropical deserts (Seager et al. 2007) and a decrease

M. R. Jury (✉)
Physics Department, UPRM, Mayagüez, Puerto Rico
e-mail: jury@uprm.edu

A. Winter
Marine Science Department, UPRM, Mayagüez, Puerto Rico

in Caribbean rainfall (IPCC 2007). Direct radiative forcing by aerosols has been shown to significantly alter tropical convective precipitation well away from emission centers by strengthening of the Northern Hadley circulation (Wong et al. 2007).

Here we describe some of the multi-disciplinary factors underlying climate change in the Caribbean, with a focus on the Hadley circulation and atmospheric composition, through an analysis of past trends in temperature, natural and man-induced aerosols and related variables in time, space and elevation. We explain the trends taking into account physical, chemical, local, and remote thermodynamic processes. The impacts of climate change are briefly reviewed and include trends in rainfall and tropical cyclones in the Caribbean.

2 Data

We utilize data from numerous sources to understand changes in air temperatures driven by the Hadley circulation and atmospheric composition (Table 1). Observed air temperatures from land station data are quality-checked, converted to standardized departures for averaging into grid boxes, then model-interpolated into the 'HadCru' data base for the Caribbean. Observations derive from Cuba, Jamaica, Haiti, Dominican Republic, Puerto Rico, Virgin Islands, Anguila, Barbuda, St Kitts & Nevis, Martinique, Dominica, St Lucia, St Vincent, and Barbados. Sea surface temperatures (SST) that are observed by ships and (since 1980) by satellites are similarly model-interpolated into a second data base. These records extend back to the beginning of the twentieth century, to enable long-term trends to be determined.

The NCEP reanalysis data model assimilates upper level temperature (T), relative humidity (RH) and winds from radiosonde stations since 1949, and infers T and RH profiles from satellite radiances since 1976. The correlation of these time series with a linear trend was analyzed per 2° grid box and then mapped in plan and section using the NOAA website www.cdc.noaa.gov/Correlation. Temperature trends over the Caribbean in the entire reanalysis period (1949+) and the satellite era (1976+) were compared, and results were found to be consistent. Although longer records are preferred, for upper level T and RH we constrain our analysis to the period since 1976, to avoid artificial trends resulting from the known discontinuity of observations (Hurrell et al. 2000). We compared radiosonde temperature data at standard levels for Puerto Rico and Barbados (from the Comprehensive Aerological Radiosonde Data Set; CARDS) (Eskridge et al. 1995) with co-located reanalysis data. Statistically significant correlations were found ($r > +0.90$), and little difference in trends could be detected.

The long-term time series were averaged over the Caribbean (14–22° N, 75–58° W), and smoothed with a 5-year running mean to isolate trends and low frequency variability. The linear trend was computed and the intercept, slope, and r^2 fit were determined. To evaluate significance, the degrees of freedom were deflated owing to autocorrelation imposed by the smoothing filter. The linear trend r^2 fit required to achieve 98% confidence is 0.25 for a ~100 year record with ~20 degrees of freedom. For the 5-month filtered satellite-era time series, $r^2 > 0.16$ is significant at 98%. Temperature data were analyzed for distribution and an r^2 value of 0.80 with respect to a second order Gaussian fit was sufficiently normal to make use of standard tests for significance.

Table 1 Information on data sets used in the analysis

Purpose	URL	Data source	Location	Comment
Land station and ship surface air temperature data	http://iridl.ldeo.columbia.edu/SOURCES/.UEA/.CRU/	Climate Research Unit of East Anglia	~2 × 2° gridded	Data has undergone a physics-based assimilation by the Hadley Center general circulation model (GCM).
Trends in upper level air temperatures, humidity and winds	http://www.cdc.noaa.gov/Correlation/	NCEP reanalysis	Various levels over the period 1949–2006	The NCEP model assimilates upper level temperature, relative humidity and winds from radiosonde stations and infers T and RH profiles from satellite radiances.
Quantify changes in the overturning Hadley circulation	IRI website	NCEP reanalysis	Vertically averaged winds over Caribbean and to south in longitudes 55–75° W	Area averages calculated for regions with statistically significant signals and consistent radiosonde data coverage, eg. 14–22° N and 4–8° N for vertical motion; and 2–12° N and 10–21° N for meridional wind.
Aerosol optical thickness (AOT)	http://iridl.ldeo.columbia.edu/SOURCES/.NASA/.GSFC/.TOMS/	NASA TOMS satellite data	~1 × 1° gridded data	AOT data analyzed for mean annual cycle by month in the area 15–20° N, 60–65° W: Puerto Rico to Barbados. Period of record 1980–2005, with gap in 1994–1995.
Satellite tropospheric ozone	http://code916.gsfc.nasa.gov/Data_services/cloud_slice/	NASA GSFC	~1 × 1° gridded data	The mean annual cycle was analyzed by averaging data by month in the Puerto Rico to Barbados region.
Analysis of future trends in temperature and rainfall	IRI website	GFDL C2.1 coupled model	2000–2100	Based on IPCC AR4 outputs using the A1B scenario

Trends in 5-month smoothed aerosol optical thickness (AOT) and tropospheric ozone (O_3) data from the TOMS satellite radiometer (1994–1995 missing) were also analyzed and compared with smoothed vegetation (NDVI) data from the AVHRR satellite radiometer in the period 1980–2006. While continuous records provide overall trends, some processes may have a seasonal dependence. Here the monthly radiosonde temperature, winds, AOT and O_3 data were analyzed for mean annual cycle in various regions, including a $5 \times 5°$ box between Puerto Rico and Barbados (15–20° N, 65–60° W).

Past observed trends were compared with future projected trends of temperature in different layers over the Caribbean using the GFDL C2.1 coupled general circulation model (GCM), run for the IPCC/AR4 assessment with the SRES A1B scenario (Meehl et al. 2007). The GFDL C2.1 model is described by Delworth et al. (2006), Gnanadeskan et al. (2006), Wittenberg et al. (2006) and Griffies et al. (2005) and is considered one of the more robust coupled GCMs that account for both climate change and variability. The period from 2001–2100 was considered and monthly projected data were 5-year smoothed and trend analyzed as above.

3 Results

3.1 Analysis of temperature and circulation trends

Century long records of observed sea (ship) and air (station) temperature exhibit significant warming trends across the Caribbean over the period 1888–2006 as illustrated in Fig. 1. The Caribbean area SST trend was 0.004°C/year, yet the 2 m air temperature trend was three times greater (0.014°C/year). The fastest rate of warming occurred at the 850 hPa level, where temperatures increased 0.029°C/year over the radiosonde era 1949–2006. The variance explained by the linear trend increases with elevation, rising from 55% at the sea surface, to 87% and 92% for the

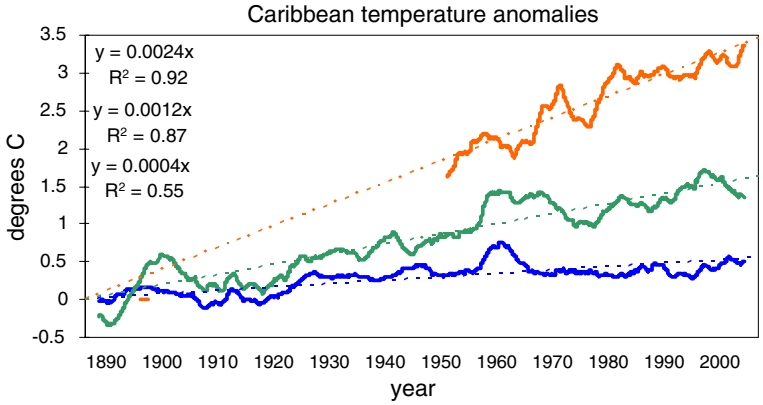

Fig. 1 Caribbean area-averaged temperature anomalies for different levels: 1,500 m (*upper*, from radiosonde), 2 m (*middle*, from land stations) and sea surface (*lower*, from ships) all smoothed with 5 year running mean. Values are offset so that the trend lines meet at $t = 0$. Linear fit and r^2 given for each series in the order they appear

2 and 1,500 m air temperature, respectively. Hence the long-term trend exceeds inter-decadal fluctuations of temperature. Wavelet spectral analysis failed to isolate any statistically significant cycles because of the trend.

Regional variations in 850 hPa air temperature (Fig. 2a) and 500 hPa vertical motion (Fig. 2b) during the satellite era were mapped over the Caribbean. Trends for 850 hPa level were positive and significant across the Caribbean, with a maximum

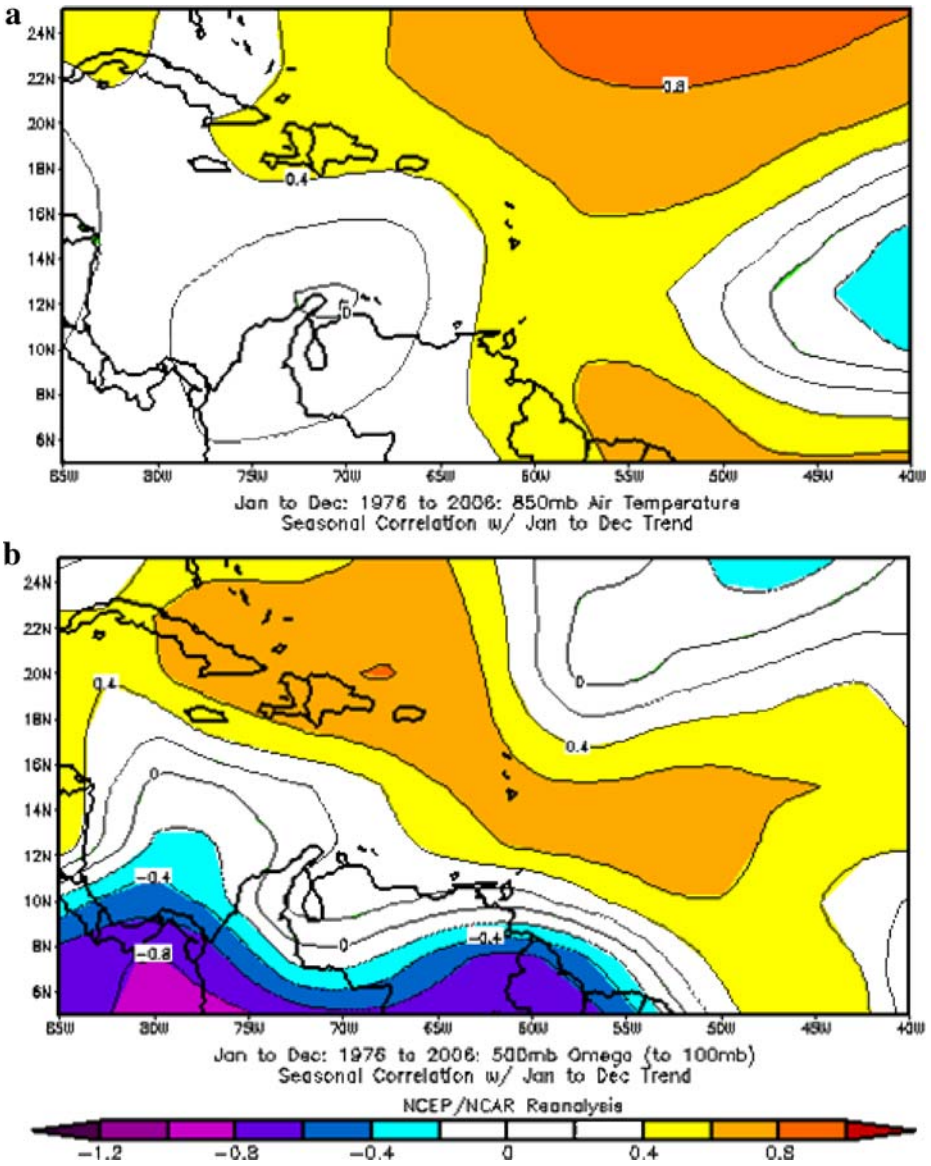

Fig. 2 Linear trend correlations for NCEP 850 hPa temperature (**a**), NCEP 500 hPa omega (**b**). Values >0.4 (*yellow*) are significant

running N–S along the eastern Antilles Islands (50–60° W). Analysis of linear trends at other levels indicates that the 700–850 hPa layer exhibited maximum warming; there was little trend above 700 hPa. An analysis of trends in different seasons reveals an increase from winter to summer, as described later. The 500 hPa layer exhibited a

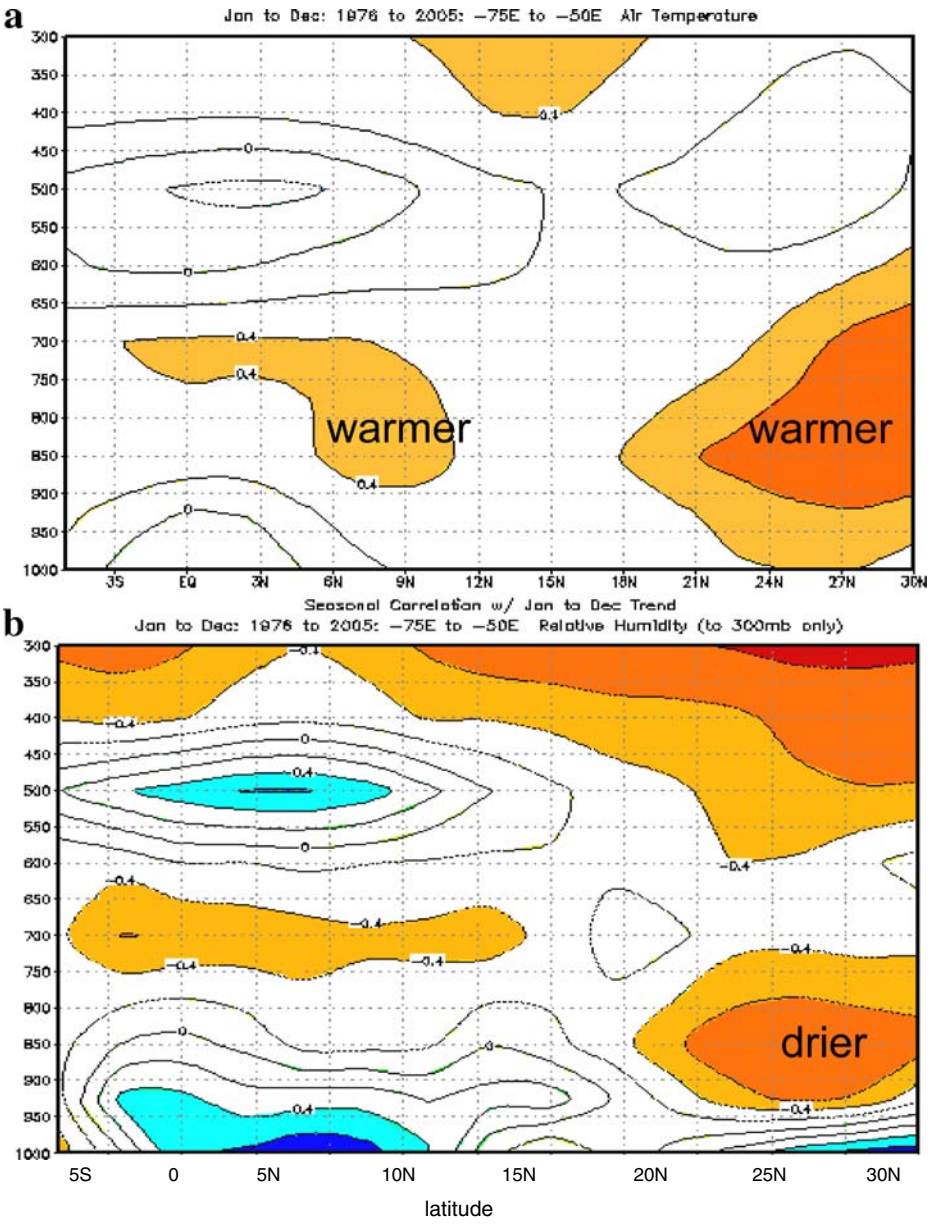

Fig. 3 **a** Trend analysis of tropical air temperature as a height-longitude section averaged over the latitude 50–75°W. $r > 0.4$ is significant >95% and shaded. **b** Trend of relative humidity as in (**a**)

broad, statistically significant NW–SE oriented axis of subsidence lying across the Caribbean. Linear trend correlation values were in the range +0.6 to +0.8 from Cuba to Barbados, indicative of accelerated sinking motions in the period 1976–2006. In the sub-tropical Atlantic trends were weak. Analysis of vertical motion trends at other levels reveal that changes in subsidence occurred over a deep layer across the Caribbean. In contrast, trends in vertical motion were reversed over northern South America and suggest an accelerating northern Hadley circulation in the longitudes 50°–70° W.

Figure 3 displays the vertical section of air temperature correlated with a linear trend, based on NCEP reanalysis data in the satellite era. The data represent averages over Caribbean longitudes, extending from northern South America to the sub-tropical Atlantic. The warming trend was greatest in the 850–700 hPa layer around 10° and 25° N (Fig. 3a). The relative humidity analysis revealed drying trends at 700 hPa over the equator, and at 850 hPa around 25° N (Fig. 3b). The drying trend extended into the upper troposphere.

Figure 4 is an analysis of trends in the Hadley circulation in a vertical north–south section extending from the Amazon across the Caribbean to the sub-tropical Atlantic. The spatial and temporal analyses reveal meridional winds accelerated from the south in the upper level and from the north in the lower level (Fig. 4a). Significant trend correlations were found in the 300 and 850–700 hPa layers over the southern Caribbean and the smoothed time series exhibit anti-phase cyclical behavior consistent with inter-decadal surges in the Hadley circulation. In Fig. 4b the vertical motion (omega) trend completes the picture of an accelerating northern

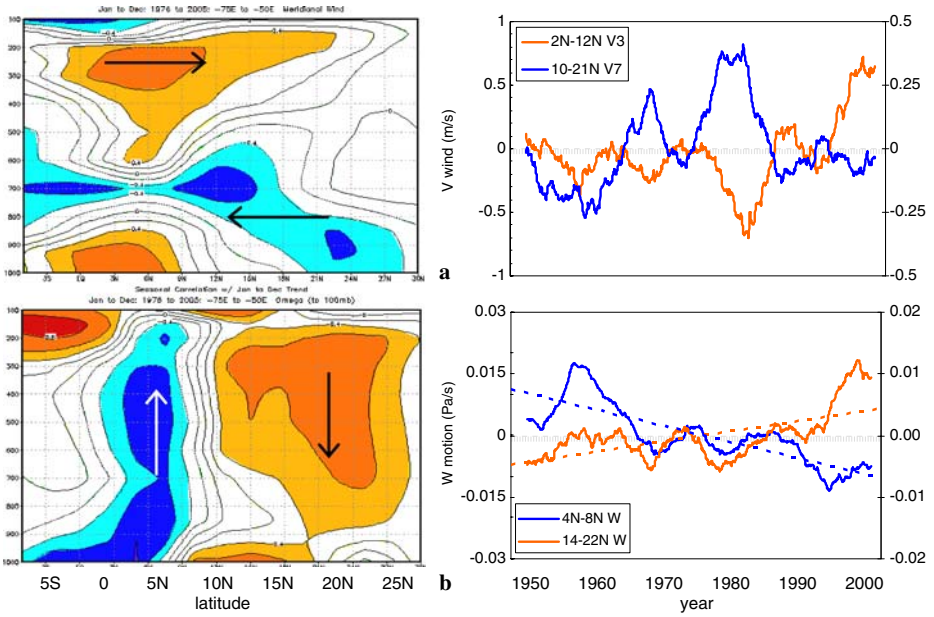

Fig. 4 **a** *Upper panels*: linear trend of meridional winds as a height-longitude section averaged over the latitude 50–75°W and time series of key areas (*right*). **b** Linear trend of vertical motion (omega) as a section and time series for key areas (*right*). *Blue curves* refer to *left hand y-axes*

Hadley circulation. A broad zone of positively trended sinking motions was found over the Caribbean, while over the northern Amazon a narrower zone of negatively trended rising motions is evident. The two time series look like a 'bow-tie' with the South American time series headed in one direction (rising, −Pa/s), and the Caribbean time series headed in the other (sinking, +Pa/s). The linear trend of rising motion over the Amazon (Caribbean) has a r^2 fit of 0.64 (0.39), significant above the 98% confidence limit.

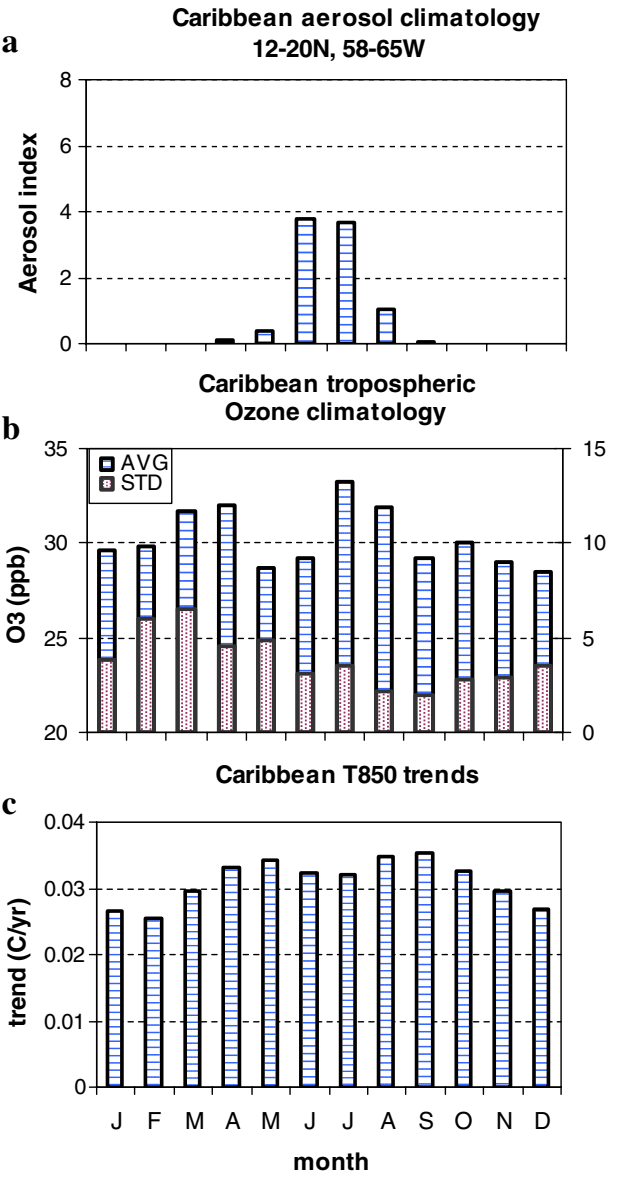

Fig. 5 **a** Aerosol and **b** ozone climatology from TOMS/NASA satellite data averaged over the eastern Caribbean. **c** 850 hPa temperature trend climatology at Barbados

3.2 Influence of atmospheric composition

Figure 5a illustrates the mean annual cycle of AOT over the eastern Caribbean. Aerosol concentrations remain low or undetectable throughout most of the year, but rise to a sharp peak in May, June and July when the Sahara desert surface is very hot and prone to dust storms. During summer the trade winds surge across the tropical Atlantic, bringing the Saharan air layer westward towards the Caribbean. In contrast, tropospheric ozone (Fig. 5b) exhibits a weak annual cycle over the Caribbean that tends to follow RH. This is attributable to the migrating character of both winds and emissions over western Africa; 700 hPa easterly flow increases during summer, while smoke fires increase during winter. Thus the two nearly cancel out, with transport slightly more important than source rate. Ozone variability over the Caribbean is greatest in March—the peak season for vegetation burning in the Sahel.

The mean annual cycle of 850 hPa temperature trends over the eastern Caribbean (Fig. 5c) has an amplitude of ~25% that peaks in early and late summer. This bi-modal shape is qualitatively matched by tropospheric O_3 (and RH) but not by AOT which has a singular peak in summer. Vegetation across the African Sahel has increased over the period 1980–2004 as the region recovered from drought, so dust plumes could be expected to decline. However tropospheric ozone over the tropical Atlantic has increased ~8% since 1980 from burning of the African savanna that releases smoke and GHGs such as CO (cf. http://mopitt.eos.ucar.edu/mopitt/data/plots/mapsv3_mon.html). Such an increase in land use could be expected from a population that has doubled from 1975 to 2000 (Openshaw 2005).

4 Discussion

Why does the trade wind inversion layer warm faster than the surface? Is it a physical mechanism or a localized greenhouse effect related to atmospheric composition? We hypothesize that air temperatures in the layer around 1,500 m (850 hPa) are rising >3 times faster than SST because of an acceleration of the meridional overturning Hadley circulation. Figure 4b shows that there is a trend toward faster sinking motions over the Caribbean accompanied by increasing northerly (southerly) lower (upper) flow to the south, connecting with uplift over South America. The sinking motions induce a faster rate of warming and drying in the trade wind inversion than at other levels, while the Amazon monsoon becomes more vigorous (Held and Soden 2006). Compression caused by sinking motion in the Hadley circulation has driven up air temperatures over the Caribbean. The African dust and smoke plume intersects this subsidence and helps focus its effects at the top of the atmospheric boundary layer (~850 hPa), resulting in a 1.5°C increase in temperature since 1950.

African dust and smoke emissions of ~100 Tg/year originate ~5,000 km east of the Caribbean, yet recent observations have found tropospheric ozone values up to 160 ppb in the east Atlantic (Hawkins et al. 2007). As the plume takes ~10 days to reach the Caribbean, much deposition leaves smaller aerosols and trace gases to act as radiative absorbers that enhance the greenhouse effect (Bergstrom et al. 2003; Sinha et al. 2003). The composition of the smoke, expressed as emission factors over West African savanna is: carbon dioxide ($\sim 10^3$), carbon monoxide ($\sim 10^2$), particulates ($\sim 10^1$), and nitrogen oxides ($\sim 10^0$). The long-lived trace gases will not

leave a regional footprint; ozone, carbon monoxide and particulates, on the other hand, are relatively short-lived and may contribute to localized radiative absorption in elevated layers, mainly of incoming shortwave radiation in 'young' plumes of particulate aerosols (near Africa) and of outgoing longwave radiation in 'old' plumes dominated by transformed GHGs.

To compare how various factors drive changes in air temperatures we employ the thermodynamic equation with terms for physical forcing and atmospheric composition: $\partial T_{850}/\partial t = (KT/p)\,\omega + 1/g\; C_p\,(\partial A/\partial p)$. The left term is the change of 850 hPa temperature with time and the right terms are heating from vertical motions and radiative absorption respectively. Horizontal temperature advection is assumed to be negligible in the tropics. Sinking motions in the 4–8 km layer over the Caribbean have increased by $\sim$1.5 10^{-2} Pa s^{-1} (Fig. 4b) yielding ΔT $\sim$0.022°C/year. Thus physical forcing accounts for about two-thirds of the trend. The internal heating rate

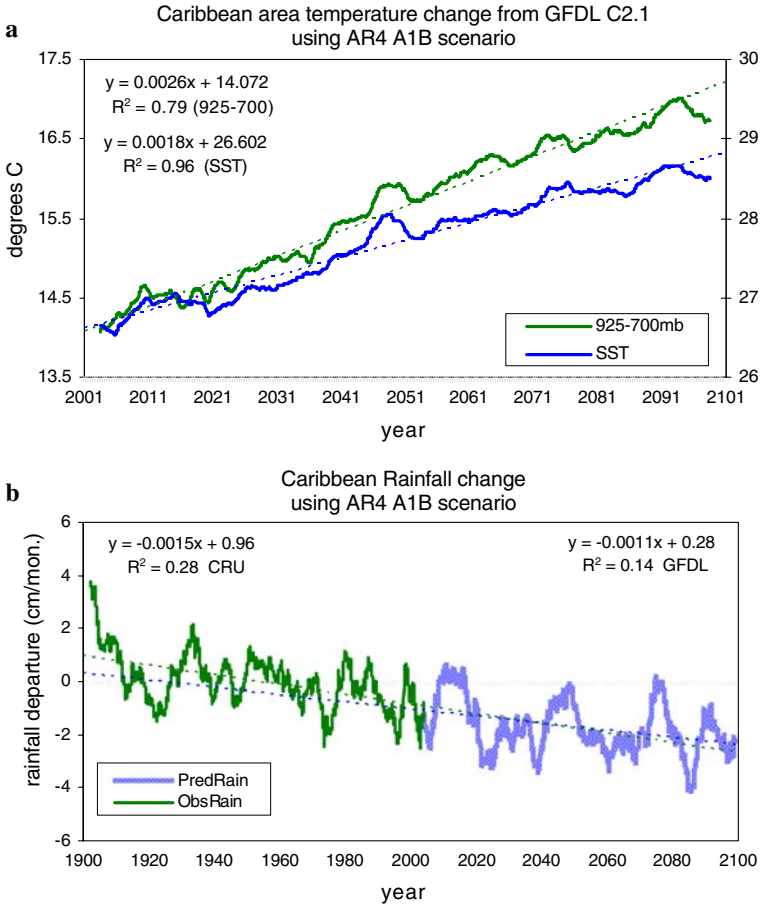

Fig. 6 **a** Projected future trends in SST and inversion layer temperatures from the GFDL C2.1 model run using the A1B scenario. **b** Comparison of past observed and future projected trends of Caribbean rainfall, revealing consistent downward trends

1/g C_p ($\partial A/\partial p$) uses gravity, specific heat capacity of air and net radiative flux across the layer (Hobbs 2000; Pilewskie et al. 2003). Layer thickness varies with season and latitude, and based on aircraft and Calipso satellite lidar data (cf. Fig. 7b) can be assumed to extend from 850–600 hPa. Given an elevated concentration of short-lived greenhouse gases including tropospheric O_3 and CO over the eastern Caribbean, a fractional absorption of ~0.7% (~7 W m^{-2}) over a volume 4 10^9 m^3 is estimated, in

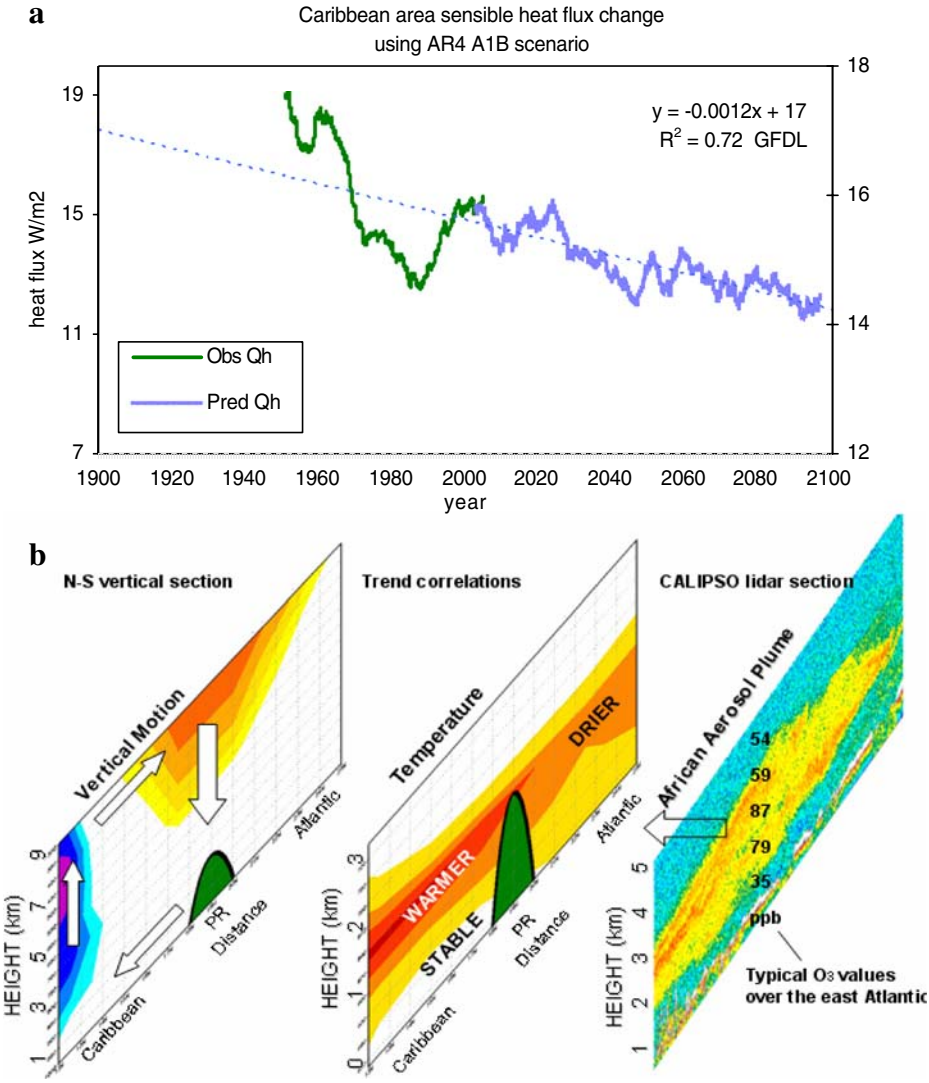

Fig. 7 **a** Past observed and future projected trends of sensible heat flux (SST minus air T times wind speed) from NCEP reanalysis and GFDL C2.1 model run using the A1B scenario. **b** Schematic of Hadley cell (*left*) and aerosol plume (*right*) interactions that produce warming in the inversion layer (*middle*), illustrated as a N–S vertical section, with correlation trends analyzed in *left panels*, and satellite aerosol concentration in *right*. Note varying *vertical scales*

concordance with Mfuamba (2007). With these assumptions, a greenhouse warming ΔT of ~0.007°C/year is calculated; providing about one-third of the observed T_{850} trend in the Caribbean.

Future projected trends of temperatures may be compared with past observed trends using the IPCC AR4 outputs (Meehl et al. 2007) from the GFDL C2.1 GCM forced with the A1B scenario over the period 2000–2100, Fig. 6a. The elevated layer has a projected temperature trend of 0.031°C/year, while the SST trend is 0.022°C/year in the Caribbean region. The model forecast is consistent with the past trend for the elevated layer (0.029°C/year from Fig. 1), but the model's surface trend is far greater than observed. The r^2 linear trend fit decreases from 0.96 at the surface to 0.79 in the elevated layer, unlike observations, but magnitudes are consistent. Again, inter-decadal fluctuations of temperature are overwhelmed by the long-term trend. Results will vary according to model and scenario used, so our choice is perhaps fortunate. It is unclear why the model fails to correctly estimate the SST trend and it is beyond the scope of this paper to consider the oceanic processes.

An important offshoot from our study is the increased stability imparted by a warming elevated layer. With air temperatures rising faster than sea temperatures, the resulting decline in surface heat flux (Fig. 7a) may limit rainfall. We investigate this using monthly CRU gridded rainfall records averaged over the Caribbean in the past 100 years, compared with GFDL C2.1 projected trends in Fig. 6b. Indeed rainfall has decreased 0.18 mm/year in the period 1900–2000 and is projected to continue decreasing at a similar rate in the next 100 years. The r^2 linear trend fit is relatively small (0.28 observed, 0.14 projected), so inter-decadal variability of rainfall exceeds its long-term change. A reassuring feature is the continuity of rainfall fluctuations from past to future. A further point of agreement is found between regional drying and reduced tropical cyclone frequency as indicated by Caribbean proxy records over the past few hundred years (Nyberg et al. 2007).

5 Summary

The northern Hadley circulation brings subsiding air over the Caribbean in conjunction with rising motion over the Amazon basin. Absorbing aerosols at the top of the boundary layer (~850 hPa) intersect this subsidence and helps focus its effects contributing to rapid warming of an elevated layer over the Caribbean. The African smoke and dust plumes that drift westward across the Atlantic enhance the greenhouse effect just above the marine boundary layer (1–3 km) following deposition of larger reflective particles. It is predominantly in eastern Caribbean longitudes that the smaller aerosols and short-lived trace gases induce radiative absorption. Even if trends in the Hadley circulation and the aerosol–GHG plumes are relatively weak, the elevated warming occurs because of their coincidence at the top of the boundary layer. The ocean, with its heat capacity and sluggish currents, is expected to lag behind the atmosphere in its response to recent changes in the earth's energy budget, and so a decline in sea-to-air heat fluxes is anticipated. A strengthened trade wind inversion and stabilized lower atmosphere will tend to counteract the more gradual warming of Caribbean SST, thereby suppressing rainfall and tropical cyclones, and contribute to a rather unique and localized response to global warming.

References

Bengtsson L, Hodges KI, Roeckner E (2006) Storm tracks and climate change. J Climate 19: 3518–3543

Bergstrom RW, Pilewskie P, Schmid B, Russell B (2003) Estimates of spectral aerosol single scattering albedo and aerosol radiative effects during Safari2000. J Geophys Res 108(13):8474

Delworth TL, Rosati A, Stouffer RJ, Dixon KW, Dunne J, Findell K, Ginoux P, Gnanadesikan A, Gordon CT, Griffies SM, Gudgel R, Harrison MJ, Held IM, Hemler RS, Horowitz LW, Klein SA, Knutson TR, Lin S-J, Milly PCD, Ramaswamy V, Schwarzkopf MD, Sirutis JJ, Stern WF, Spelman MJ, Winton M, Wittenberg AT, Wyman B (2006) GFDL's CM2 global coupled climate models. Part I: formulation and simulation characteristics. J Climate 19(5):643–674

Eskridge RE, Alduchov O, Chernykh IV, Zhai P, Polansky AC, Doty SR (1995) A comprehensive aerological reference data set (CARDS): rough and systematic errors. Bull Am Meteorol Soc 76:1759–1775

Frierson DM, Lu WJ, Chen G (2007) Width of the Hadley cell in simple and comprehensive general circulation models. Geophys Res Lett 34:L18804. doi:10.1029/2007GL031115

Fu X, Wang B, Tao L (2006) Satellite data reveal the 3-D moisture structure of tropical intraseasonal oscillation and it's coupling with underlying ocean. Geophys Res Lett 33:L03705. doi:10.1029/2005GL025074

Gnanadeskan A, Dixon KW, Griffies SM, Balaji V, Barreiro M, Beesley JA, Cooke WF, Delworth TL, Gerdes R, Harrison MJ, Held IM, Hurlin WJ, Lee H-C, Liang Z, Nong G, Pacanowski RC, Rosati A, Russell J, Samuels BL, Song Q, Spelman MJ, Stouffer RJ, Sweeney CO, Vecchi G, Winton M, Wittenberg AT, Zeng F, Zhang R, Dunne JP (2006) GFDL's CM2 global coupled climate models. Part 2, basline ocean simulation. J Climate 19:675–697

Griffies SM, Gnanadesikan A, Dixon KW, Dunne JP, Gerdes R, Harrison MJ, Rosati A, Russell JL, Samuels BL, Spelman MJ, Winton M, Zhang R (2005) Formulation of an ocean model for global climate simulations. Ocean Sci 1:45–79

Hawkins MD, Morris VR, Nalli NR, Joseph E (2007) Comparison of aeroso1 and ozone profiles within Saharan dust and biomass burning plumes. Proc AMS Conf Atmos Chem Austin J7.9

Held IM, Soden BJ (2006) Robust responses of the hydrological cycle to global warming. J Climate 19–21:5686–5699

Hobbs PV (2000) Introduction to atmospheric chemistry. Cambridge Univ Press, New York

Hurrell JW, Brown SJ, Trenberth KE, Christy JR (2000) Comparison of tropospheric temperatures from radiosondes and satellites: 1979–98. Bull Am Meteorol Soc 81:2165–2177

IPCC (2007) Physical science basis. In: Solomon S et al (eds) 4th assessment report of the intergovernmental panel on climate change. Cambridge Univ Press, New York, 996 pp

Meehl GA, Covey C, Delworth T, Latif M, McAvaney B, Mitchell JFB, Stouffer RJ, Taylor KE (2007) The WCRP CMIP3 multimodel dataset: a new era in climate change research. Bull Am Meteorol Soc 88:383–1394

Mfuamba J-P (2007) Tropospheric ozone climatology at Brazzaville. MSc thesis, Univ. K.Z.Natal, Durban, 88 pp

Nyberg J, Malmgren BA, Winter A, Jury MR, Kilbourne KH, Quinn TM (2007) Low atlantic hurricane activity in the 1970s-80s compared to the past 270 years. Nature 447:698–701

Openshaw K (2005) Natural resources, population growth and sustainable development in Africa. In: Low P-S (ed) Climate change and Africa. Cambridge Univ Press, Cambridge, pp 113–123

Pilewskie P, Pommier J, Bergstrom R, Gore W, Howard S, Rabbette M, Schmid U, Hobbs PV, Tsay SC (2003) Solar spectral radiative forcing during SARARI2000. J Geophys Res 108(D13): 8486

Seager R, Ting M, Held I, Kushnir Y, Lu J, Vecchi G, Huang H-P, Harnik N, Leetmaa A, Lau N-C, Li C, Velez J, Naik N (2007) Model projections of an imminent transition to a more arid climate in Southwestern North America. Science. doi:10.1126/science.1139601

Sinha P, Hobbs PV, Yokelson RJ, Bertschi IT, Blake DR, Simpson IJ, Gao S, Kirchstetter TW, Novakov T (2003) Emissions of trace gases and particles from savanna fires in southern Africa. J Geophys Res 108(d13):8487. doi:10.1029/2002JD002325

Wittenberg AT, Rosati A, Lau N-C, Ploshay JJ (2006) GFDL's CM2 global coupled climate models. Part III: tropical pacific climate and ENSO. J Climate 19(5):698–722

Wong S, Dessler AE, Colarco PR, dsSilva A (2007) The instability associated with the cross-Atlantic transport of Saharan dust and its meteorological implications. Proc AMS Conf Atmos Chem Austin J7.8